

High redshift Gamma-ray Bursts

Ruben Salvaterra

INAF/IASF-Milan, via E. Bassini 15, I-20133 Milano, Italy

email: ruben@lambrate.inaf.it

Abstract

Ten years of operations of the *Swift* satellite have allowed us to collect a small sample of long Gamma-Ray Bursts (GRBs) at redshift larger than six. I will review here the present status of this research field and discuss the possible use of GRBs as a fundamental new tool to explore the early Universe, complementary to quasar and galaxy surveys.

Keywords:

gamma-ray burst: general, cosmology: observations, dark ages, reionization, first stars

1. Introduction

In the standard Λ CDM scenario, the first stars, the so-called Population III (PopIII) stars, are predicted to form in dark matter minihalos of typical mass $\sim 10^6 M_{\odot}$ at $z \sim 20 - 30$ out of a gas of pristine composition (see Ciardi & Ferrara, 2005; Bromm & Yoshida, 2011, for recent reviews). Thanks to their peculiar chemical composition, they are expected to be more massive than the subsequent stellar populations with typical mass of $\sim 40 M_{\odot}$ (Hosokawa et al., 2011), possibly extending up to hundred solar masses (Hirano et al., 2014). The formation of these stars mark the fundamental transition from a simple, very homogeneous Universe to the complex and structured one we see already in place a billion years after the Big Bang. During this period of time two fundamental transitions are expected to occur: (i) a change in the SFR mode, i.e. from massive PopIII to solar-size PopII/I stars and (ii) the cosmic reionization, i.e. the change of the inter-galactic medium (IGM) from a neutral to a fully ionized state. There is a general consensus that the first transition is driven by the so-called chemical feedback (Schneider et al., 2002), i.e. the enrichment of star forming clouds by the first supernova explosions above a critical threshold of $Z_{\text{crit}} = 10^{5 \pm 1} Z_{\odot}$ (Schneider et al., 2003). As the chemical feedback is essentially a local effect, on cosmological scale the two populations should be coeval for a long period of time (Schneider et al., 2006; Tornatore et al., 2007; Maio et al., 2010). Understanding how and when the change in the SFR mode happened is one of the main goals for current studies of galaxy formation in the early

Universe and the detection of PopIII stars one of the main challenges of the next generation of space and ground facilities (see Bromm & Yoshida, 2011, for a review). The cosmic reionization of the IGM has been extensively studied in the last years both from a theoretical and observational point of view (see Loeb & Furlanetto, 2013, for a recent review). While many steps towards our understanding of reionization process have been done, still many fundamental details are missed: In which way does it proceed? How gradual and how prolonged was the process? Was radiation from early stars sufficient to sustain this phase transition? Do PopIII stars or quasars have a major role in driving the process? Is some other more exotic process at work? etc.

Historically, the exploration of the distant Universe has been carried out following two main pathways: the observations of bright quasars detected in wide shallow surveys (Fan, 2012), and of distant galaxies identified through the drop-out technique in small fields (Bouwens et al., 2014). Thanks to their extreme brightness Gamma-Ray Bursts (GRBs) represent an alternative way to access those early epochs. As demonstrated by GRB 090423 at $z = 8.2$ (Salvaterra et al., 2009; Tanvir et al., 2009), they can be detected even at distances much larger than any other cosmic object. In principle, their afterglow emission can be observed up to $z \sim 20$ (Ciardi & Loeb, 2000; Gou et al., 2004) providing useful information about the ionization and metal enrichment history of the early Universe. Here, I will review the present observational status of this research field and discuss the possible role of GRBs in the explo-

ration of the Universe during and before the reionization epoch.

This paper is organized as follows. In Section 2, a brief summary of the observations of the GRBs at $z > 6$ and of their host galaxies is given. Section 3 presents the expected rate of high- z GRBs both from PopII and PopIII stars and the expected properties of the relative host galaxies. In Section 4, the use of GRBs as a probe of the early Universe is reviewed. Finally in Section 5 I present some ideas for the future of this research field. The conclusions are drawn in Section 6.

2. Observations

2.1. The Swift high- z GRB sample

In ten years of operations *Swift* has detected a handful of bursts with spectroscopically confirmed redshift larger than 6. In addition, other three GRBs have well constrained photometric redshift above this limit. The observed high- z sample represents $\sim 1\%$ of all *Swift* bursts, $\sim 2.5\%$ of those with known z . The main properties of the $z > 6$ GRB sample are given in Table 1.

- **GRB 050904** at $z=6.3$ Kawai et al. (2006)

This burst was firstly imagined by the 25-cm telescope TAROT (Klotz et al., 2005). Its high- z nature was recognized by multi-wavelength photometric data (Haislip et al., 2006; Tagliaferri et al., 2005) and firmly confirmed spectroscopically three days after the *Swift* trigger by the Subaru telescope (Kawai et al., 2006). The afterglow spectrum provided an upper limit on the neutral hydrogen fraction at the GRB redshift of $x_{\text{HI}} < 0.17$ at 1σ confidence (Totani et al., 2006) and a measure of the metallicity at the level of $\sim 0.1 Z_{\odot}$ (Kawai et al., 2006). Recently, Thöne et al. (2013) revised this value, inferring a slightly lower metallicity from the S II $\lambda 1243$ equivalent width, resulting in $\log(Z/Z_{\odot}) = -1.6 \pm 0.3$. The afterglow spectral energy distribution (SED) requires the presence of SMC or supernova (SN) type dust at a level of $A_V = 0.15 \pm 0.07$ (Stratta et al. 2011 but see Zafar et al. 2011b). The modeling of afterglow data from X-ray to radio suggests GRB 050904 to be an energetic burst blowing up in a dense medium with $n \simeq 680 \text{ cm}^{-3}$ (Frail et al., 2006; Laskar et al., 2014).

- **GRB 080913** at $z = 6.7$ (Greiner et al., 2009)

The high- z nature of this burst was recognized via the detection of a spectral break between the i'

and z' bands of the GROND instrument and then confirmed spectroscopically by VLT observations. The analysis of the red damping wing constrained $x_{\text{HI}} < 0.73$ at 90% confidence level (Patel et al., 2010). In spite of the rapid follow-up campaign, the faintness of the afterglow prevented the detection of any metal absorption line, but the $\text{S II} + \text{Si II}$ at 2.9σ level (Patel et al., 2010). Dust absorption of $A_V = 0.12 \pm 0.03$ is found from SED fitting (Zafar et al., 2011a).

- **GRB 090423** at $z = 8.2$ (Salvaterra et al., 2009; Tanvir et al., 2009)

The spectroscopic redshift of this burst was secured by TNG (Salvaterra et al., 2009) and by VLT (Tanvir et al., 2009), and still represents the distance record for a cosmic object. Radio observations by VLA were reported by Chandra et al. (2010). The analysis of the multi-wavelength dataset show that the afterglow is reminiscent of many other lower redshift bursts, suggesting that in spite of its extreme redshift, its progenitor and the medium in which it blew up were not peculiar. Indeed, its detection is consistent with the high- z tail of PopII/I GRB redshift distribution (Salvaterra et al., 2009). From the X-ray to optical SED no absorption by dust is evident with $A_V < 0.1$ (Salvaterra et al. 2009; Tanvir et al. 2009, but see Laskar et al. 2014).

- **GRB 130606A** at $z = 5.9$ (Chornock et al., 2013; Castro-Tirado et al., 2013; Totani et al., 2014; Hartoog et al., 2014)

The redshift of this burst was obtained by Gemini-North (Chornock et al., 2013), GTC (Castro-Tirado et al., 2013), Subaru (Totani et al., 2014) and VLT (Hartoog et al., 2014). In particular, the superior resolution and wavelength coverage of the VLT/X-shooter instrument showed the potentiality of GRBs as tool to study in great details the metal enrichment of star forming region inside high- z galaxies (Hartoog et al., 2014). Precise column densities of H, Al, Si and Fe are reported together with limit on C, O, S and Ni. The host metallicity is constrained to be in the range of 0.03-0.06 solar and the high [Si/Fe] in the host suggests the presence of dust depletion (though $A_V < 0.05$ from SED fitting). The best fit of the $\text{Ly}\alpha$ absorption line is obtained for $\log(N_{\text{HI}}) = 19.94 \pm 0.01$ and negligible neutral hydrogen in the external medium, with $x_{\text{HI}} < 0.03$ at 3σ significance.

GRB	z	E_p [erg]	E_{iso} [erg]	$\log(N_{\text{HI}})$ [cm $^{-2}$]	$\log(N_{\text{H,X}})$ [10 21 cm $^{-2}$]	Z [Z_{\odot}]	A_V	$M_{\text{UV,host}}$ [AB]	SFR_{host} [$M_{\odot}\text{yr}^{-1}$]
050904	6.3	3178	1.24×10^{54}	21.6	63^{+34}_{-29}	-1.6 ± 0.3	0.15 ± 0.07	> -19.95	< 4.1
080913	6.7	1008	7×10^{52}	19.84	95^{+89}_{-77}	-	0.12 ± 0.03	> -19.00	< 1.3
090423	8.2	746	1.88×10^{53}	-	102^{+49}_{-54}	-	< 0.1	> -16.95	< 0.38
130606A	5.9	2028	2.7×10^{53}	19.93	< 30	-1.35 ± 0.15	< 0.05	-	-
140515A	6.3	376	5.1×10^{52}	18.62	< 226	< -0.8	0.11 ± 0.02	-	-
090429B	9.4	437	4.31×10^{52}	-	140 ± 10	-	0.10 ± 0.02	> -19.65	< 2.4
120521C	6.0	-	1.9×10^{53}	-	< 60	-	< 0.05	-	-
120923A	8.5	376	5.1×10^{52}	-	< 720	-	-	-	-

Table 1: List of the GRBs at $z > 6$ detected by *Swift* and of their observed properties: peak energy (E_p), isotropic equivalent energy in the 1-10000 keV range (E_{iso}), hydrogen column density in the host (N_{HI}), X-ray equivalent hydrogen column density ($N_{\text{H,X}}$), host metallicity (Z) and dust extinction (A_V). The last two columns report the limits on the host galaxy luminosity ($M_{\text{UV,host}}$) and SFR. See text for references.

- **GRB 140515A** (Chornock et al., 2014; Melandri et al., 2015)

The redshift of this burst has been secured by Gemini-North (Chornock et al., 2014), GTC and VLT (Melandri et al., 2015). Chornock et al. (2014) analysed the Gemini-North spectra finding no evidence of narrow absorption lines, indicating a host metallicity $Z < 0.15 Z_{\odot}$. However, Melandri et al. (2015) by modeling the X-ray to optical SED found evidence for dust absorption to the level of $A_V \sim 0.1$ indicating some metal enrichment. The red damping wing of Lyman- α can be fitted equally well by a single host galaxy absorber with $\log(N_{\text{HI}}) = 18.62 \pm 0.08$ or a pure IGM absorption with neutral hydrogen fraction $x_{\text{HI}} \sim 0.06$ (Chornock et al., 2014).

Other three GRBs have accurate photometric redshift measurement that place in the $z > 6$ sample:

- **GRB 090429B** at $z \sim 9.4$ (Cucchiara et al., 2011)

Cucchiara et al. (2011) collected the afterglow data obtained with Gemini-North, VLT and GROND. In the best fit model these data are all consistent with a photometric redshift of $z = 9.4$ and low extinction $A_V = 0.10 \pm 0.02$. A secondary solution at very low redshift is still allowed by the SED fitting, but it seems unlikely due to the lack of any detection of the GRB host galaxy (see next Section).

- **GRB 120521C** at $z \sim 6$ (Laskar et al., 2014)

The large multi-wavelength dataset of the afterglows lead to $z \simeq 6.0$ also supported by the analysis of the very low signal-to-noise Gemini-North spectrum. All afterglow data after ~ 0.25 days can be

well fitted assuming constant-density medium with $n_0 \sim 0.05 \text{ cm}^{-3}$ and no dust extinction, $A_V < 0.05$. The radio observations revealed the existence of a jet break corresponding to an jet angle $\theta_{\text{jet}} \simeq 3$ degrees. An isotropic energy $E_{\text{iso}} = 1.9 \pm 0.8 \times 10^{53}$ erg is obtained by extrapolating the BAT fluence.

- **GRB 120923A** at $z \sim 8.5$ (Tanvir, 2013)

The optical-NIR afterglow of this burst was imaged by Gemini-North telescope ~ 1.4 hours after the *Swift* trigger. The blue IR color, H-K ~ 0.1 mag together with the break between the Y- and J-band is suggestive of a strong high- z candidate (Levan et al., 2012). The fit to all photometric data gives $z \sim 8.5$ (Tanvir, 2013). No radio or mm detection is reported.

2.2. General properties of high- z GRBs

In spite of the burst to burst differences and of the small size of the sample, some interesting clues about the nature of high- z bursts can be gathered by comparing them with bursts at lower redshifts. Thus, in the following, I will compare the properties of $z > 6$ bursts with those of a well selected, complete sample of bright *Swift* bursts (BAT6, Salvaterra et al., 2012). The BAT6 sample has been selected only on the basis of the γ -ray peak flux as seen by *Swift*/BAT and is characterized by a very high completeness in redshift (95%, Salvaterra et al., 2012; Covino et al., 2013). Thus, it represents a perfect sub-sample to compare the results of the high- z burst population with.

The top-left panel of Fig. 1 shows the position of $z > 6$ bursts in the $E_p - E_{\text{iso}}$ plane. The black points represents the BAT6 sample (Nava et al., 2012) and the shaded area shows the 3σ scatter around the $E_p - E_{\text{iso}}$

correlation. High- z bursts nicely follow the Amati correlation suggesting that their prompt emission properties do not differ significantly from bright lower- z bursts. This consistency calls for a common central engine (and progenitor star).

In the top-right panel of Fig. 1 I have then compared the rest-frame 2-10 keV light curves normalized for the corresponding E_{iso} of $z > 6$ bursts with those obtained from the BAT6 sample (D’Avanzo et al., 2012). Indeed, the X-ray light curves of low- z GRBs tend to cluster when such a normalization is performed and strong correlation between L_X and E_{iso} is found at early times. This effect is seen also in high- z GRBs and their X-ray light curves can not be distinguished from those of low- and intermediate- z bursts. This conclusion is also supported by more extensive, although model dependent, analysis of afterglow emission. It has been shown (Chandra et al., 2010; Laskar et al., 2014) that the total energy, microphysical parameters and medium properties of the high- z GRBs are in line with those derived for lower redshift bursts.

In the bottom-left panel of Fig. 1, the available host dust extinction estimates for $z > 6$ bursts are plotted against those obtained for the BAT6 sample (Covino et al., 2013). Being selected only on the basis of the GRB γ -ray peak flux, the BAT6 sample is representative of the extinction distribution in GRB selected galaxies: 50% of bursts suffer less than 0.3-0.4 mag extinction and only 13% of GRBs have $A_V > 2$ mag. The high- z sample is characterized by little or no absorption¹, suggesting a decrease in dust content in star-forming environments at high redshifts (Zafar et al., 2011a). Similarly, the metallicities inferred for $z \sim 6$ bursts are in line, though at the lower end, with the distribution of Z measured in lower redshift GRB afterglows (Savaglio et al., 2009; Sparre et al., 2014). The observed Z and A_V values (or limits) are indeed in agreement with those expected for high- z galaxies populating the faint end of the luminosity function (see e.g. Salvaterra et al., 2011).

At variance with lower redshift bursts, all high- z GRBs have measured (or limit consistent with) very high X-ray equivalent hydrogen column densities, $N_{\text{H,X}}$ (bottom-right panel of Fig. 1). At lower redshift, a high $N_{\text{H,X}}$ is usually connected to highly extinguished afterglows (Campana et al., 2012; Covino et al., 2013). However, at higher redshifts this interpretation seems to be unrealistic given our knowledge of galaxy evo-

lution at early times. Moreover, little or no dust absorption is found in high- z bursts, calling for unusual metal-to-dust ratios. In recent years, a well defined trend of increasing $N_{\text{H,X}}$ with redshift has been found using both GRBs and AGNs (Campana et al., 2010; Behar et al., 2011; Starling et al., 2013; Campana et al., 2015). High- z GRBs extend this relation to higher redshifts quite nicely with no $N_{\text{H,X}}$ value or limit below the observed lower envelope. Campana et al. (2015) have shown, by means of dedicated numerical simulations, that this effect can be naturally explained by the absorption of intervening metals along the line-of-sight (LOS), being the observed lower envelope due to metals present in the IGM. An additional contribution in most of the LOSs comes from metals in the diffuse gas in galaxy groups at $z \sim 0 - 2$.

In conclusion, high- z GRBs do not show any peculiar feature with respect to low- and intermediate- z events. Both the energetics and the afterglow properties are found to be very similar. The medium in which they blow up does not differ too much in terms of density, metallicity and dust content. Finally, also the duration of their prompt emission is consistent with those of the low- z sample taking into account cosmological and instrumental effects (Littlejohns et al., 2013). All these findings support the idea that the GRBs detected so far at $z > 6$ represent the high redshift tail of the PopII/I GRB redshift distribution.

2.3. High- z GRB host galaxies

In the last few years, deep searches with both ground- and space-based facilities (Tanvir et al., 2012; Basa et al., 2012; Walter et al., 2012; Berger et al., 2014) have been carried out searching for the host galaxy of high- z GRBs. Indeed, the a-priori, precise knowledge of the position and distance of the galaxy provided by the GRB detection allows to optimize the telescope setup, pushing the instruments to their limit.

Tanvir et al. (2012) reported the observation of the field of four GRBs at $z > 6$ with HST with filters chosen to cover the rest-frame wavelength range 1200-1500Å, i.e. above the Lyman- α . In spite of the very deep limits reached (see Table 1), none of the targets have been identified. Similar results were obtained by Basa et al. (2012) using slightly shallower VLT observations. More recently, Berger et al. (2014) imaged the field of GRB 090423 with *Spitzer* at 3.6 μm and ALMA at 222 GHz, but, also in this case, no detection is reported. These results imply that all the hosts lie below the characteristic luminosity value at their respective redshifts, with star formation rates $\text{SFR} < 4 M_{\odot} \text{yr}^{-1}$ in all cases. In particular, GRB 090423 was possible to

¹However, the lack of highly extinguished bursts may reflect a bias in the sample as even a small amount of absorption at $z > 6$ will prevent the detection of the optical afterglow and thus of the redshift measure.

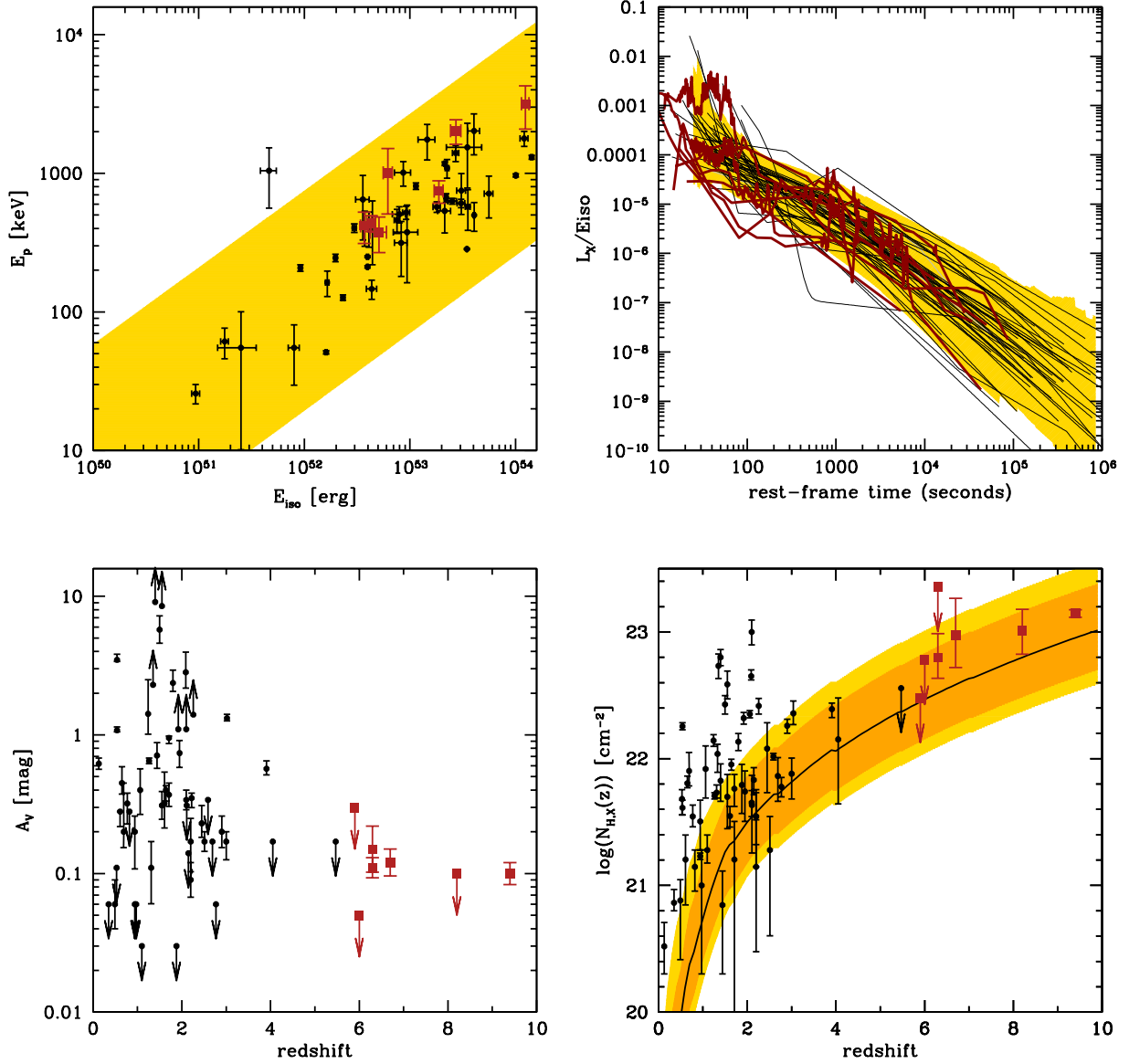


Figure 1: Comparison of the properties of $z > 6$ bursts (red squares and lines) with those of a well selected complete sub-sample of bright *Swift* GRB, the BAT6 sample (black points and lines; Salvaterra et al. (2012)). *Top-left panel:* $E_p - E_{\text{iso}}$ correlation where BAT6 bursts are from Nava et al. (2012). The shaded regions represents the 3σ scatter around the best-fitting relation. *Top-right panel:* rest-frame 2-10 keV light curves normalized to their isotropic energy where BAT6 data are from D’Avanzo et al. (2012). The shaded region represents the 2σ scatter around the mean value of the L_X/E_{iso} distributions at the given rest-frame time. *Bottom-left panel:* dust extinction as a function of redshift, where BAT6 data are from Covino et al. (2013). *Bottom-right panel:* intrinsic X-ray equivalent hydrogen column densities $N_{\text{H,X}}$ as a function of redshift, where BAT6 data are from Campana et al. (2012). The shaded regions represent the effect of intervening material along the line-of-sight (see Campana et al. 2015 for the details).

derive a strong limit on the unobscured $\text{SFR} < 0.38 M_{\odot} \text{ yr}^{-1}$ (Tanvir et al., 2012), while the ALMA non detection required the obscured SFR to be $< 5 M_{\odot} \text{ yr}^{-1}$ (Berger et al., 2014).

Tanvir et al. (2012) also stacked all images deriving a limit on the mean SFR per galaxy of $< 0.17 M_{\odot} \text{ yr}^{-1}$, consistent with the idea that the bulk of star formation activity is missed in current deep HST surveys (Salvaterra et al., 2011). Moreover, these findings offer independent evidence that the galaxy luminosity function is evolving rapidly with redshift with a steeper faint-end slope or with a decreasing characteristic luminosity at high redshift (Tanvir et al., 2012).

3. Theory

3.1. The high- z GRB population

As described in previous Section, *Swift* has detected almost one GRB at $z > 6$ per year. Considering the 1.4 sr field of view of the BAT instrument, this corresponds to a rate² of $\sim 0.6 \text{ bursts yr}^{-1} \text{ sr}^{-1}$. It is worth to ask whether such a rate is expected on the basis of our knowledge of the intrinsic GRB redshift distribution and luminosity function (Bromm & Loeb, 2002; Daigne et al., 2006; Salvaterra & Chincarini, 2007; Salvaterra et al., 2009b; Butler et al., 2010; Wanderman & Piran, 2010; Robertson & Ellis, 2012; Salvaterra et al., 2012; Ghirlanda et al., 2015).

Figure 2 shows the distribution of peak fluxes of bursts at $z > 6$ as measured in the 15-150 keV *Swift*/BAT band. The histogram is compared with the model results under different assumptions on the evolution of the GRB luminosity function (Salvaterra et al., 2012). The models have been calibrated by jointly fitting the differential peak flux distribution of BATSE long GRBs and the redshift distribution of the BAT6 sample. The models reproduce the rate and peak flux distribution of $z > 6$ burst remarkably well³ with a small excess in the predicted population at the faintest fluxes. However, since, in general, to faint γ -ray fluxes correspond faint optical afterglows (e.g. Melandri et al., 2014), some high- z faint bursts can be missed being the detection of its afterglow difficult even with 8-m class telescopes.

²While this represents a lower limit, given the fact that some high- z burst can be among GRBs without redshift measurement, it should be noted that there is a possible positive bias at work here. Indeed, most of the observational programs at large ground- and space-facilities have as their primary goal the detection of high- z events.

³Since the BAT6 sample is limited to $z < 5.4$ there is no assumption in the model about the peak flux distribution of $z > 6$ GRBs

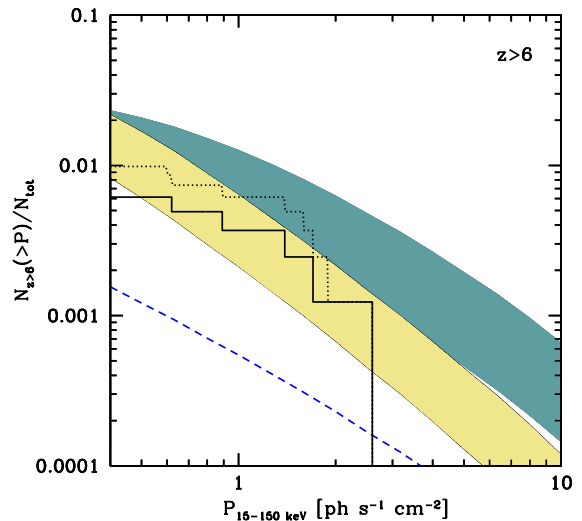


Figure 2: Peak flux distribution of bursts at $z > 6$ as measured in the 15-150 keV *Swift*/BAT band. The solid (dotted) histogram shows the distribution of bursts with spectroscopic (spectroscopic and photometric) redshift. The shaded regions report model predictions (Salvaterra et al., 2012), taking into account the uncertainties in the determination of the GRB luminosity function and evolution. Dark (light) color refers to the density (luminosity) evolution models. The dashed line is obtained assuming no evolution and clearly underestimates the number of high- z detections at all peak fluxes.

By extrapolating model results to fainter fluxes (Salvaterra et al., 2008; Ghirlanda et al., 2015), it can be shown that bursts $z > 6$ represent $\sim 10\%$ of the whole population, suggesting that GRBs are quite efficient in selecting high- z objects. The detection of these events is one of the main goals of any future GRB mission.

3.2. GRBs from PopIII stars

Different authors (Mészáros & Rees, 2010; Komissarov & Barkov, 2010; Suwa & Ioka, 2011; Toma et al., 2011; Nagakura et al., 2012; Nakauchi et al., 2012; Piro et al., 2014) have proposed that the conditions for jet breakout could be met also during the final phases of the collapse of a PopIII massive star. Although under different frameworks, all models consistently predict PopIII GRBs to be very energetic events, with total energies exceeding by orders of magnitude those expected in PopII events. In particular Toma et al. (2011) suggested that PopIII bursts could have an equivalent isotropic energy $\sim 10^{56-57}$ erg making their detection possible even at the highest redshifts. A much longer prompt emission, with typical duration of 10^4 s, is also foreseen in most of the models. However, all these characteristics are shared observationally with the population of ultra-long GRBs

recently detected at much lower redshift (Levan et al., 2014) and likely associated with PopII blue supergiant stars (Nakauchi et al., 2013). Thus, they do not represent a unique feature to firmly identify a PopIII event. Strong evidence could be provided by the absence of metal absorption lines in the afterglow spectrum down to a level of the critical metallicity. However, the measure of such low metallicity (or a limit consistent with it) requires extremely high signal-to-noise spectra that can be even beyond the capabilities of 30-m class telescopes. In the absence of any other observational tool to identify PopIII events, radio observations can provide an important clue. Indeed extremely powerful radio afterglows (Ciardi & Loeb, 2000; Toma et al., 2011; Ghirlanda et al., 2013b) are expected given the peculiar energetics of PopIII events. Ghirlanda et al. (2013b) showed that PopIII radio afterglows should reside in a very distinct position in observed peak time-peak flux plane, reaching much larger peak fluxes at later times than any PopII GRBs.

We have seen in Section 2.2 that it is unlikely that the observed $z > 6$ bursts are associated with PopIII progenitors. This piece of information has been used to put a limit on the expected rate of PopIII events (Bromm & Loeb, 2006; Campisi et al., 2011; Toma et al., 2011; de Souza et al., 2011; Maio & Barkov, 2014; Mesler et al., 2014). By means of dedicated numerical simulations including the effect of the chemical feedback, Campisi et al. (2011) computed the expected redshift distribution of PopIII GRBs. The PopIII GRB rate is found to increase from $z = 20$ to $z = 8 - 10$ and then it decreases rapidly becoming negligible at $z \sim 5$. Under the assumption that all PopIII GRBs can be detected by *Swift*⁴, the maximum allowed rate is $\sim 0.03 \text{ Gpc}^{-3} \text{ yr}^{-1}$. Assuming a typical jet angle of ~ 7 degree and a typical PopIII mass of $\sim 100 M_{\odot}$, this corresponds to < 1 PopIII GRB every 500 PopIII stars, comparable with the PopII/SN type Ib/c ratio (Ghirlanda et al., 2013a).

In conclusion, even if GRBs can really result from the collapse of a massive PopIII star, they will be extremely rare with $< 0.05 \text{ event yr}^{-1} \text{ sr}^{-1}$ at $z > 6$. PopIII GRBs become the dominant observed population only at $z > 10 - 15$ (Campisi et al., 2011). On the other hand, even a single detection of a GRB powered by PopIII stars, i.e. a extremely high- z , very energetic, long event with a bright radio afterglow peaking at late times, would

⁴This may be not the case since the *Swift* trigger algorithm (Lien et al., 2014) is not very sensitive to extremely long GRBs.

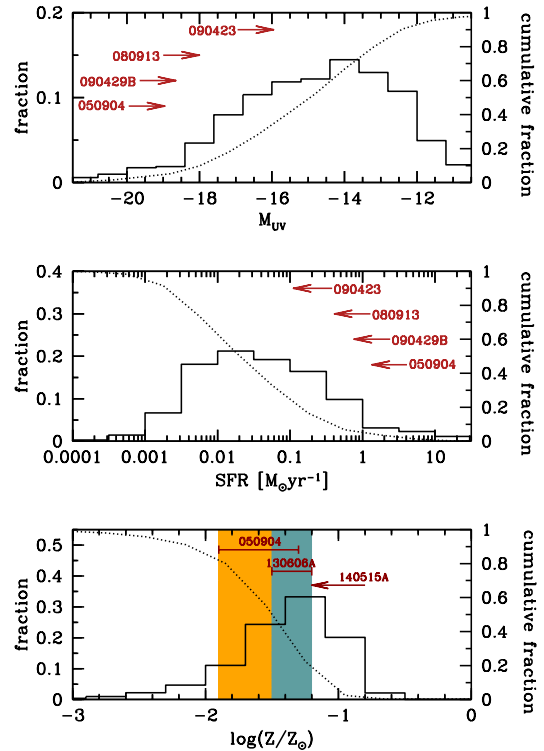


Figure 3: Properties of simulated GRB hosts in the redshift range $z = 6 - 10$. Panels from top to bottom show the distribution of UV absolute magnitude, of the SFR (in $M_{\odot} \text{ yr}^{-1}$), and of gas phase metallicities (in solar units). The dotted line shows the normalized cumulative distributions (see right y-axis). The arrows in the first two panels report the limits on M_{UV} and SFR of GRB hosts (Tanvir et al., 2012). The shaded areas in the bottom panel correspond to the metallicity measured in the GRB 050904 (Thöne et al., 2013) and GRB 130606A (Hartoog et al., 2014) afterglow spectrum. The arrow shows the limit inferred for GRB 140515A (Chornock et al., 2014).

represent a breakthrough in the study of the first generation of stars.

3.3. High- z GRB host galaxies

In absence of any detection (see Section 2.3), the relation of GRB selected galaxies with the typical high- z galaxy population has been studied by means of dedicated semi-analytical models (Trenti et al., 2012) or numerical simulations (Salvaterra et al., 2013; Elliott et al., 2015).

Salvaterra et al. (2013) derived the expected properties of the GRB hosts at $z = 6 - 10$ by means of cosmological numerical simulations including all relevant feedback effects at these redshifts. GRBs are found to explode in bursty galaxies with typical star formation rates $\text{SFR} \approx 0.03 - 0.3 M_{\odot} \text{ yr}^{-1}$, stellar masses $M_{\star} \approx 10^6 - 10^8 M_{\odot}$, specific star formation rates

$s\text{SFR} \approx 3 - 10 \text{ Gyr}^{-1}$. The distribution of their UV luminosities (see top panel of Fig. 3) places them in the faint end of the galaxy luminosity function, below the capabilities of current instruments. This is consistent with the lack of detection and suggests that deep observations with the James Webb Space Telescope (JWST) are required to pinpoint them. Finally, the bulk of the GRBs are found to explode in galaxies already enriched with metal to $Z \approx 0.03 - 0.1 Z_{\odot}$ (bottom panel of Fig. 3), consistently with the metallicity inferred in $z \sim 6$ GRB afterglow spectra (Salvaterra et al. 2013, but see Cen & Kimm 2014).

The same simulations allow to predict the properties of host galaxies of PopIII GRB events (Campisi et al., 2011). These bursts are found to reside typically in objects at the lower end of the stellar mass with $M_{\star} < 10^7 M_{\odot}$ as they have the higher probability of having still a pristine composition. While a metallicity below Z_{crit} is obviously required in the star forming cloud from which the PopIII GRB arises, some of the PopIII GRB hosts are found in galaxies with $Z \sim 10^{-3} Z_{\odot}$. This may reflect the fact that some PopIII event can be associated with pockets of metal-free gas in the outskirts of an enriched galaxy (Tornatore et al., 2007).

4. High- z GRBs as a tool

4.1. Independent measure of the SFR

It is well established that long GRBs are associated to the death of massive stars (see Hjorth & Bloom, 2012, and references therein). Therefore, they should trace to some extent the star formation activity through cosmic times and they can be used to measure in an independent way the global SFR (Kistler et al., 2009; Ishida et al., 2011; Robertson & Ellis, 2012). In this respect, GRBs have many advantages compared with usual probes: (i) they are detected at higher redshifts; (ii) they are independent on the galaxy brightness; (iii) they do not suffer of usual biases affecting optical/NIR surveys. Indeed, although hampered by small statistics, the detection of the few high- z GRBs already suggests that the global SFR at $z \approx 8 - 9$ is 3-5 times higher than deduced from high- z galaxy searches through the drop-out technique (Ishida et al., 2011). An important caveat to be mentioned here is that GRBs may be not perfect tracers of the SFR. Indeed, in order to reproduce the redshift distribution of bursts detected by *Swift* (e.g. Salvaterra & Chincarini, 2007; Wanderman & Piran, 2010; Robertson & Ellis, 2012; Salvaterra et al., 2012), some kind of evolution with redshift is required. Thus, a precise knowledge of the nature and the value of this bias is needed to properly

use GRBs as SFR probe in the early Universe. This can be achieved by measuring the GRB LF and its evolution at low and intermediate redshifts (Salvaterra et al., 2012; Wanderman & Piran, 2010; Pescalli et al., 2015) and by studying well selected sample of low- z GRB host galaxies (Boissier et al., 2013; Perley et al., 2013; Hunt et al., 2014; Trenti et al., 2014; Vergani et al., 2014). In particular, Vergani et al. (2014) have shown that the stellar mass distribution of a small, but complete, sample of GRB selected galaxies at $z < 1$ is consistent with the existence of a mild metallicity bias in the GRB hosts, with bursts forming more efficiently in environments with $Z < 0.3 - 0.5 Z_{\odot}$ (Vergani et al., 2014). If these findings are confirmed by larger samples, GRBs can be considered good tracers of the SFR at least at $z > 3 - 4$.

4.2. The reionization history

Similar to quasars, GRBs have been used to measure the neutral hydrogen fraction in the IGM by fitting the red damping wing of the Ly α and therefore to place strong constraints on the reionization redshift (Totani et al., 2006; Chornock et al., 2013; Totani et al., 2014; Hartoog et al., 2014; Chornock et al., 2014). With respect to quasars, GRBs have many advantages: (i) they are already detected at much larger redshift than quasars; (ii) they reside in average cosmic regions, less affected by local ionization effects or clustering, and (iii) their spectrum follows a power-law making continuum determination much easier. The main limitation of this method is represented by the presence of the host galaxy absorption (McQuinn et al., 2008), although this can be in principle separated being less extended. Chen et al. (2007) found that $\sim 20 - 30\%$ of GRBs have small enough hydrogen column density to allow a direct measure of absorption from a partially neutral IGM. Moreover, the typical N_{HI} value for GRB hosts is expected to decrease with increasing redshift (Nagamine et al., 2008). This idea is now supported by the fact that three out of the four $z > 6$ GRBs for which the intrinsic HI column density has been measured, showed $N_{\text{HI}} < 10^{20} \text{ cm}^{-2}$ (see Table 1). In particular, a very low N_{HI} is found in the case of GRB 140515A (Chornock et al., 2014) suggesting that a statistical sample of bursts with low intrinsic column densities can be gathered in future allowing to firmly constrain the reionization process.

Another effective method to constrain the reionization history is based on the statistics of peaks/gaps in the afterglow spectrum between Ly α and Ly β , i.e. corresponding to transmission/absorption regions along the LOS (Paschos & Norman, 2005). Gallerani et al.

(2008) have shown that the distribution of the dimension of the largest dark gap is sensitive to the assumed reionization history provided that a statistical sample of ~ 20 LOSs is gathered.

Finally, the study of the HI forest over-imposed on the GRB radio afterglow with SKA of a very high redshift burst could offer, in principle, a powerful tool to study the reionization process (Xu et al., 2011; Ciardi et al., 2015). However, it requires the detection of an extremely bright radio afterglow at the level of ~ 10 mJy at $z > 7 - 8$, that may be possible in the case of PopIII GRBs.

Beside constraining the reionization history and its variance along different LOSs, GRBs can provide an estimate of the typical escape fraction of UV photons from early galaxies. The measure of this crucial quantity from the observation of the escaping Lyman continuum radiation is already very difficult at $z \sim 3$ (Vanzella et al., 2012), and may be impossible for the small, faint galaxies responsible for the bulk of star formation at $z > 6$. A statistical sample of GRBs provide an alternative way to infer it from the distribution of N_{HI} over many LOSs. Useful constrains have so far obtained at $z = 2 - 4$ with $f_{\text{esc}} < 7.5\%$ (Fynbo et al., 2009), being higher redshift studies prevented by the small statistic of the sample. The measure of the escape fraction from typically star-forming galaxies during the epoch of reionization will provide the missing piece of the puzzle in our understanding of how galaxies reionize the IGM.

4.3. Studying high- z galaxies

Theoretical models and observational evidence suggests that most of the UV photons that reionize the Universe are emitted by low mass, faint galaxies missed even in the deepest observations by HST. The detection of these objects is one of the main scientific goal of the next generation of space telescopes. However, little or no information about the physical properties (e.g. metal and dust content) of these objects will be accessible even with JWST. High- z GRBs can provide a useful, complementary tool to investigate the building up of metals at these early stages of galaxy formation and, in particular, in those objects that provide the bulk of the ionizing photons (Salvaterra et al., 2013). Indeed, GRB events are produced by the same massive stars that emit the FUV photons able to ionize hydrogen. Metal absorption line observations of a large sample of good signal-to-noise GRB spectra will allow to recover the cosmic metal enrichment history, to extend the mass-metallicity and FMR to higher redshift (Salvaterra et al., 2013; Laskar et al., 2011), to perform stellar population studies (Grieco et al., 2014; Ma et al., 2015), and

to search for peculiar nucleosynthesis pattern (see next Section).

Metal absorption lines over-imposed to the afterglow radiation have been already detected even $z > 6$ showing that high- z galaxies are already enriched to a few percent solar. In particular, the spectrum of GRB 130606A obtained with VLT/X-shooter (Hartoog et al., 2014) shows a great variety of metal elements allowing accurate abundance and gas kinematic studies of the inner region of a $z \sim 6$ galaxy. Even better and richer datasets will be gathered when the 30-m class telescope like E-ELT will become operative. These studies can be complemented by X-ray spectroscopic observations of bright GRBs with the next generation of X-ray instruments (Campana et al., 2011). In particular, with the Athena satellite (Nandra et al., 2013) it will become possible to directly measure the abundance patterns in X-ray afterglows allowing, in principle, to discriminate between different nucleosynthesis sources (Jonker et al., 2013).

Beside metal absorption lines, the observation of H_2 molecular absorption and of the local dust law can provide further details about the host enrichment. As discussed in Section 2.2, evidence of dust extinction in four $z > 6$ GRBs has been derived by studying the X-ray-to-optical SED. Furthermore, in the case of GRB 140515A dust depletion is suggested by the peculiar metal abundance ratio (Hartoog et al., 2014). These observations show that GRBs can provide fundamental clues about the presence of dust in high- z galaxies. Moreover, they can be used to constrain the dust formation channels at work at those early epoch. It is interesting to note that for GRB 071025 at $z \sim 5$ (Perley et al., 2010) and tentatively for GRB 050904 at $z = 6.3$ (Stratta et al., 2011) evidences for SN synthesized dust has been reported. Tracking the dust enrichment history of first galaxies is also very important for better understand the PopIII/PopII transition. Indeed, it has been shown that even a little amount of dust in the medium will induce the formation of low mass stars (Schneider et al., 2003, 2012).

4.4. Indirect search for PopIII stars

PopIII GRBs (if any) are expected to be extremely rare and difficult to distinguish from other GRB populations (see Section 3.2). An indirect, but fruitful, way to search for the elusive PopIII stars is represented by the study of the metal and dust composition of the ISM of distant galaxies enlightened by PopII GRBs. Indeed, peculiar metal abundance ratios (Heger & Woosley, 2002) and dust composition (Schneider et al., 2004) are foreseen as the result of the

enrichment of first massive SN explosions. The detection of such a signature in the optical-NIR afterglow of a very high- z GRBs will provide a strong evidence for the existence of very massive ($> 100 M_{\odot}$) PopIII stars.

Wang et al. (2012) found that PopIII enriched gas will result in much larger equivalent widths of metal absorption lines than typical PopII enrichment. Moreover, Ma et al. (2015) showed that in principle the [C/O] and [Si/O] alone could be enough to distinguish a PopIII enriched environment, although, in practice, the detection of more elements (such as S and Fe) is needed. PopII GRBs exploding in a PopIII enrichment medium are expected to be rare at $z = 6$ ($< 1\%$ of the GRB population at that redshift) but the probability to find them increases with z being $\sim 10\%$ at $z = 10$ (Ma et al., 2015). They should reside in small host galaxies with $M_{\star} \sim 10^{5-6} M_{\odot}$ and $Z < 10^{-2.8} Z_{\odot}$. Thus, the detection of a $z > 10$ burst with a metallicity below this threshold will be a strong candidate to be either a PopIII event or a PopII GRBs blowing up in a PopIII enriched medium.

4.5. Others

For the sake of completeness (see McQuinn et al., 2009; Amati et al., 2013, for a more complete list) I would like to briefly mention here some other possible uses of GRBs in the study of early Universe:

- *constrain the dark matter particle* (Mesinger et al., 2005; de Souza et al., 2013). The redshift distribution of GRBs can set limits on the dark matter particle mass, m_{χ} . Using a sub-sample of $z > 4$ GRBs $m_{\chi} > 1.6 - 1.8$ keV at 95% confidence level is found.

- *non-Gaussianity* (Maio et al., 2012). Deviations from Gaussianity of the primordial density field will translate in different rates of GRBs $z \gg 6$. A single GRB detection at $z > 15$ will favor non-Gaussian scenarios with a positive non-linear parameter.

- *radiation field* (Inoue et al., 2010; Kakuwa et al., 2012). The ultraviolet intergalactic radiation field below the Lyman edge energy can cause attenuation in the γ -ray spectra of GRBs. This may be observable at high- z by the Cherenkov Telescope Array (CTA).

- *magnetic fields* (Takahashi et al., 2011). Pair echoes from luminous high- z GRBs may be detectable with CTA providing a unique probe of weak intergalactic magnetic fields at early stages of structure formation.

5. Present and future of the fields

The detection of high- z GRBs is one of the main goals driving the design of the next GRB missions (Amati et al., 2013). As already discussed, GRBs are

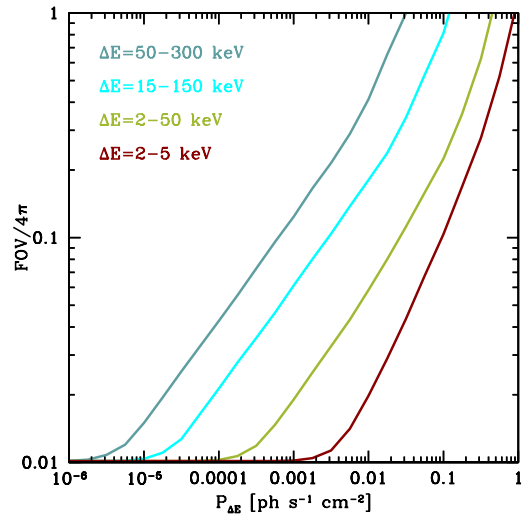


Figure 4: Required sensitivity, in terms of minimum peak flux $P_{\Delta E}$ that can be detected in the given energy band ΔE , and field-of-view to detect 10 GRB yr^{-1} at $z > 8$. Different lines correspond to different energy bands as labeled in the plot, i.e. to different mission concept. See Ghirlanda et al. (2015) for the details of the calculation.

very effective in selecting high- z objects and sufficiently bright to be detectable up to beginning of the star formation activity. While the forthcoming SVOM satellite (Godet et al., 2012) or the proposed LOFT mission (Amati et al., 2015) will surely increase the $z > 6$ GRB sample, it is also clear that in order to full exploit the potentiality of GRBs as a probe of the early Universe, a much larger sample of well studied, high- z GRBs should be collected.

Due to redshift scaling, in the observer frame the prompt emission of high- z GRBs is expected to peak at softer energies than lower redshift bursts. However, as the sensitivity of current GRB satellites allow us to detect only the bright-end of the GRB LF at high- z , the mean observed peak energy is $\langle E_{p,obs} \rangle \sim 150$ keV similar to low- z bursts. Therefore, while a facility operating in the soft X-rays will be, in general, more efficient in selecting high- z GRBs, a much better sensitivity than current instruments should also be foreseen.

The scientific goals outlined in the previous section call for a large statistical sample of well studied high- z GRBs. To be competitive with other probes, at least a hundred of GRBs at $z > 6$ with several tens of them lying at $z > 8$ should be detected. Ghirlanda et al. (2015) computed the expected detection rate of high- z GRBs by a generic detector with defined energy band and sensitivity by means of an observational tested population synthesis model of long GRBs. Following the results of

this work, Figure 4 shows the sensitivity and field-of-view of a mission able to detect 10 GRBs yr⁻¹ at $z > 8$ and operating in different energy bands. For instance, by adopting the *Swift* sensitivity of $\sim 0.4 \text{ ph s}^{-1} \text{ cm}^{-2}$ and energy band, we can see that the goal is never reached. On the other hand, limiting ourselves to the *Swift* FOV of 1.4 sr, a hundred times better sensitivity than *Swift* is needed. A X-ray instrument will instead require a sensitivity of $0.1 \text{ ph s}^{-1} \text{ cm}^{-2}$ in the 2-5 keV band for the same FOV. It is worth to note that the same mission will also detect thousands of bursts at lower redshifts (plus other transients). In order to effectively select high- z candidates, the presence of a 0.5-1 m infrared telescope on-board should be foreseen (together with fast repointing capabilities). This instrument will allow not only to promptly measure the redshift but also to perform low-resolution ($R \sim 1000$) spectroscopic studies (e.g. to identify metal absorption lines) when the afterglow is at the maximum of its brightness. A rapid dissemination of best high- z candidates is also fundamental in order to trigger follow-up observations by future facilities operating at different wavelengths: optical-NIR (E-ELT, JWST if still operating), radio (SKA), X-ray (ATHENA), TeV (CTA).

In conclusion, the study of the high- z Universe with GRBs requires a X-ray detector with unprecedented combination of sensitivity and FOV coupled with an infrared telescope to select reliable high- z candidates. The THESEUS mission recently proposed for the M4 ESA call matches all these characteristics.

6. Conclusions

In this paper, I have briefly reviewed the status and the prospect for the exploration of the high redshift Universe with GRBs. A few solid considerations can be drawn:

- (i) GRBs do exist at very high redshift and can be detected and studied with present-day facilities;
- (ii) high- z GRBs are very similar to low- and intermediate- z ones;
- (iii) GRBs are an efficient way to select high- z objects;
- (iv) high- z GRBs are hosted in faint galaxies that are missed even in the deepest surveys;
- (v) high- z GRBs have proved to be an independent and powerful tool to study the early Universe.

Although the current sample is limited to a few bursts, future dedicated missions can provide a sufficiently large number of GRBs at $z > 6$ to study the first bound structures in a complementary way with respect to galaxy and quasar surveys.

Acknowledgments

This research was supported by the ASI-INAF contract (1/005/11/1). The author would like to thank A. Melandri for providing the X-ray light curve for the $z > 6$ sample, S. Campana for providing the measure of the $N_{\text{H,X}}$ for some of the high- z bursts, G. Ghirlanda for providing the E_{iso} values and the expected rate of GRBs at $z > 8$.

References

References

- Amati L. et al., 2013, arXiv:1306.5259
Amati L. et al., 2015, arXiv:1501.02772
Basa S., Cuby J. G., Savaglio S., Boissier S., Clément B., Flores H., Le Borgne D., Mazure A., 2012, *A&A*, 542, A103
Behar E., Dado S., Dar A., Laor A., 2011, *ApJ*, 734, 26
Berger E. et al., 2014, *ApJ*, 796, 96
Boissier S., Salvaterra R., Le Floc'h E., Basa S., Buat V., Prantzos N., Vergani S. D., Savaglio S., 2013, *A&A*, 557, A34
Bouwens R. J. et al., 2014, *ApJ*, 793, 115
Bromm V., Loeb A., 2002, *ApJ*, 575, 111
Bromm V., Loeb A., 2006, *ApJ*, 642, 382
Bromm V., Yoshida N., 2011, *ARA&A*, 49, 373
Butler N. R., Bloom J. S., Poznanski D., 2010, *ApJ*, 711, 495
Campana S., Salvaterra R., Ferrara A., Pallottini A., 2015, *A&A*, 575, A43
Campana S. et al., 2012, *MNRAS*, 421, 1697
Campana S., Salvaterra R., Tagliaferri G., Kouveliotou C., Grindlay J., 2011, *MNRAS*, 410, 1611
Campana S., Thöne C. C., de Ugarte Postigo A., Tagliaferri G., Moretti A., Covino S., 2010, *MNRAS*, 402, 2429
Campisi, M. A., Maio, U., Salvaterra, R., Ciardi, B., 2011, *MNRAS*, 416, 2760
Castro-Tirado A. J. et al., 2013, arXiv:1312.5631
Cen R., Kimm T., 2014, *ApJ*, 794, 50
Chandra P. et al., 2010, *ApJ*, 712, L31
Chen H.-W., Prochaska J. X., Gnedin N. Y., 2007, *ApJ*, 667, L125
Chornock R., Berger E., Fox D. B., Lunnan R., Drout M. R., Fong W.-f., Laskar T., Roth K. C., 2013, *ApJ*, 774, 26
Chornock R., Berger E., Fox D. B., Fong W., Laskar T., Roth K. C., 2014, arXiv:1405.7400
Ciardi B., Ferrara A., 2005, *ssr*, 116, 625
Ciardi B., Inoue S., Mack K. J., Xu Y., Bernardi G., 2015, arXiv:1501.04425
Ciardi B., Loeb A., 2000, *ApJ*, 540, 687
Covino S. et al., 2013, *MNRAS*, 432, 1231
Cucchiara A. et al., 2011, *ApJ*, 736, 7
Daigne F., Rossi E. M., Mochkovitch R., 2006, *MNRAS*, 372, 1034
D'Avanzo P. et al., 2012, *MNRAS*, 425, 506
de Souza R. S., Yoshida N., Ioka K., 2011, *A&A*, 533, A32
de Souza R. S., Mesinger A., Ferrara A., Haiman Z., Perna R., Yoshida N., 2013, *MNRAS*, 432, 3218
Elliott J., Khochfar S., Greiner J., Dalla Vecchia C., 2015, *MNRAS*, 446, 4239
Fan X., 2012, *Research in Astronomy and Astrophysics*, 12, 865
Frail D. A. et al., 2006, *ApJ*, 646, L99
Fynbo J. P. U. et al., 2009, *ApJS*, 185, 526
Gallerani S., Salvaterra R., Ferrara A., Choudhury T. R., 2008, *MNRAS*, 388, L84

- Ghirlanda G. et al., 2013a, MNRAS, 428, 1410
Ghirlanda G. et al., 2013b, MNRAS, 435, 2543
Ghirlanda G. et al., 2015, MNRAS, 448, 2514
Godet O. et al., 2012, SPIE, 8443, 1
Gou L. J., Mészáros P., Abel T., Zhang B., 2004, ApJ, 604, 508
Greiner J. et al., 2009, ApJ, 693, 1610
Grieco V., Matteucci F., Calura F., Boissier S., Longo F., D'Elia V., 2014, MNRAS, 444, 1054
Haislip J. B. et al., 2006, Nature, 440, 181
Hartoog O. E. et al., 2014, arXiv:1409.4804
Heger A., Woosley S. E., 2002, ApJ, 567, 532
Hirano S., Hosokawa T., Yoshida N., Umeda H., Omukai K., Chiaki G., Yorke H. W., 2014, ApJ, 781, 60
Hjorth J., Bloom J. S., 2012, The Gamma-Ray Burst - Supernova Connection, Cambridge University Press, pp. 169–190
Hunt L. K. et al., 2014, A&A, 565, A112
Hosokawa T., Omukai K., Yoshida N., Yorke H. W., 2011, Science, 334, 1250
Inoue S., Salvaterra R., Choudhury T. R., Ferrara A., Ciardi B., Schneider R., 2010, MNRAS, 404, 1938
Ishida E. E. O., de Souza R. S., Ferrara A., 2011, MNRAS, 418, 500
Jonker P. et al., 2013, arXiv:1306.2336
Kakuwa J., Murase K., Toma K., Inoue S., Yamazaki R., Ioka K., 2012, MNRAS, 425, 514
Kawai N. et al., 2006, Nature, 440, 184
Kistler M. D., Yüksel H., Beacom J. F., Hopkins A. M., Wyithe J. S. B., 2009, ApJ, 705, L104
Klotz A., Boer M., Atteia J. L., 2005, GRB Coordinates Network, 3917, 1
Komissarov S. S., Barkov M. V., 2010, MNRAS, 402, L25
Laskar T., Berger E., Chary R.-R., 2011, ApJ, 739, 1
Laskar T. et al., 2014, ApJ, 781, 1
Levan A. J., Perley D. A., Tanvir N. R., Cucchiara A., 2012, GRB Coordinates Network, 13802, 1
Levan A. J. et al., 2014, ApJ, 781, 13
Lien A., Sakamoto T., Gehrels N., Palmer D. M., Barthelmy S. D., Graziani C., Cannizzo J. K., 2014, ApJ, 783, 24
Littlejohns O. M., Tanvir N. R., Willingale R., Evans P. A., O'Brien P. T., Levan A. J., 2013, MNRAS, 436, 3640
Loeb A., Furlanetto S. R., 2013, The First Galaxies in the Universe. Princeton University Press
Ma Q., Maio U., Ciardi B., Salvaterra R., 2015, MNRAS in press, arXiv:1503.01118
Maio U., Ciardi B., Dolag K., Tornatore L., Khochfar S., 2010, MNRAS, 407, 1003
Maio U., Salvaterra R., Moscardini L., Ciardi B., 2012, MNRAS, 426, 2078
Maio U., Barkov M. V., 2014, MNRAS, 439, 3520
McQuinn M., Lidz A., Zaldarriaga M., Hernquist L., Dutta S., 2008, MNRAS, 388, 1101
McQuinn M. et al., 2009, in Astronomy, Vol. 2010, astro2010: The Astronomy and Astrophysics Decadal Survey, p. 199
Melandri A. et al., 2014, A&A, 565, A72
Melandri A. et al., 2015, in preparation
Mesinger A., Perna R., Haiman Z., 2005, ApJ, 623, 1
Mesler R. A., Whalen D. J., Smidt J., Fryer C. L., Lloyd-Ronning N. M., Pihlström Y. M., 2014, ApJ, 787, 91
Mészáros P., Rees M. J., 2010, ApJ, 715, 967
Nagakura H., Suwa Y., Ioka K., 2012, ApJ, 754, 85
Nagamine K., Zhang B., Hernquist L., 2008, ApJ, 686, L57
Nakauchi D., Kashiyama K., Suwa Y., Nakamura T., 2013, ApJ, 778, 67
Nakauchi D., Suwa Y., Sakamoto T., Kashiyama K., Nakamura T., 2012, ApJ, 759, 128
Nandra K. et al., 2013, arXiv:1306.2307
Nava L. et al., 2012, MNRAS, 421, 1256
Paschos P., Norman M. L., 2005, ApJ, 631, 59
Patel M., Warren S. J., Mortlock D. J., Fynbo J. P. U., 2010, A&A, 512, L3
Perley D. A. et al., 2010, MNRAS, 406, 2473
Perley D. A. et al., 2013, ApJ, 778, 128
Pescalli A., Ghirlanda G., Salafia O. S., Ghisellini G., Nappo F., Salvaterra R., 2015, MNRAS, 447, 1911
Piro L. et al., 2014, ApJ, 790, L15
Robertson B. E., Ellis R. S., 2012, ApJ, 744, 95
Salvaterra R., Campana S., Chincarini G., Covino S., Tagliaferri G., 2008, MNRAS, 385, 189
Salvaterra R., Guidorzi C., Campana S., Chincarini G., Tagliaferri G., 2009b, MNRAS, 396, 299
Salvaterra R., Chincarini G., 2007, ApJ, 656, L49
Salvaterra R. et al., 2009, Nature, 461, 1258
Salvaterra R., Ferrara A., Dayal P., 2011, MNRAS, 414, 847
Salvaterra R. et al., 2012, ApJ, 749, 68
Salvaterra R., Maio U., Ciardi B., Campisi M. A., 2013, MNRAS, 429, 2718
Savaglio S., Glazebrook K., Le Borgne D., 2009, ApJ, 691, 182
Schneider R., Ferrara A., Natarajan P., Omukai K., 2002, ApJ, 571, 30
Schneider R., Ferrara A., Salvaterra R., Omukai K., Bromm V., 2003, Nature, 422, 869
Schneider R., Ferrara A., Salvaterra R., 2004, MNRAS, 351, 1379
Schneider R., Salvaterra R., Ferrara A., Ciardi B., 2006, MNRAS, 369, 825
Schneider R., Omukai K., Limongi M., Ferrara A., Salvaterra R., Chieffi A., Bianchi S., 2012, MNRAS, 423, L60
Sparre M. et al., 2014, ApJ, 785, 150
Stratta G., Gallerani S., Maiolino R., 2011, A&A, 532, A45
Starling R. L. C., Willingale R., Tanvir N. R., Scott A. E., Wiersema K., O'Brien P. T., Levan A. J., Stewart G. C., 2013, MNRAS, 431, 3159
Suwa Y., Ioka K., 2011, ApJ, 726, 107
Takahashi K., Inoue S., Ichiki K., Nakamura T., 2011, MNRAS, 410, 2741
Tagliaferri G. et al., 2005, A&A, 443, L1
Tanvir N. R., 2013, arXiv:1307.6156
Tanvir N. R. et al., 2012, ApJ, 754, 46
Tanvir N. R. et al., 2009, Nature, 461, 1254
Thöne C. C. et al., 2013, MNRAS, 428, 3590
Toma K., Sakamoto T., Mészáros P., 2011, ApJ, 731, 127
Tornatore L., Ferrara A., Schneider R., 2007, MNRAS, 382, 945
Totani T. et al., 2014, PASJ, 66, 63
Totani T., Kawai N., Kosugi G., Aoki K., Yamada T., Iye M., Ohta K., Hattori T., 2006, PASJ, 58, 485
Trenti M., Perna R., Levesque E. M., Shull J. M., Stocke J. T., 2012, ApJ, 749, L38
Trenti M., Perna R., Jimenez R., 2014, arXiv:1406.1503
Vanzella E. et al., 2012, MNRAS, 424, L54
Vergani S. D. et al., 2014, arXiv:1409.7064
Walter F. et al., 2012, ApJ, 752, 93
Wanderman D., Piran T., 2010, MNRAS, 406, 1944
Wang F. Y., Bromm V., Greif T. H., Stacy A., Dai Z. G., Loeb A., Cheng K. S., 2012, ApJ, 760, 27
Xu Y., Ferrara A., Chen X., 2011, MNRAS, 410, 2025
Zafar T., Watson D., Fynbo J. P. U., Malesani D., Jakobsson P., de Ugarte Postigo A., 2011a, A&A, 532, A143
Zafar T., Watson D. J., Tanvir N. R., Fynbo J. P. U., Starling R. L. C., Levan A. J., 2011b, ApJ, 735, 2